^{18}F-FLT PET During Radiotherapy or Chemoradiotherapy in Head and Neck Squamous Cell Carcinoma Is an Early Predictor of Outcome

Bianca A.W. Hoeben*[1], Esther G.C. Troost*[1], Paul N. Span[1], Carla M.L. van Herpen[2], Johan Bussink[1], Wim J.G. Oyen[3], and Johannes H.A.M. Kaanders[1]

[1]Department of Radiation Oncology, Radboud University Nijmegen Medical Centre, Nijmegen, The Netherlands; [2]Department of Medical Oncology, Radboud University Nijmegen Medical Centre, Nijmegen, The Netherlands; and [3]Department of Nuclear Medicine, Radboud University Nijmegen Medical Centre, Nijmegen, The Netherlands

This prospective study used sequential PET with the proliferation tracer 3′-deoxy-3′-^{18}F-fluorothymidine (^{18}F-FLT) to monitor the early response to treatment of head and neck cancer and evaluated the association between PET parameters and clinical outcome. **Methods:** Forty-eight patients with head and neck cancer underwent ^{18}F-FLT PET/CT before and during the second and fourth weeks of radiotherapy or chemoradiotherapy. Mean maximum standardized uptake values for the hottest voxel in the tumor and its 8 surrounding voxels in 1 transversal slice ($SUV_{max(9)}$) of the PET scans were calculated, as well as PET-segmented gross tumor volumes using visual delineation (GTV_{VIS}) and operator-independent methods based on signal-to-background ratio (GTV_{SBR}) and 50% isocontour of the maximum signal intensity ($GTV_{50\%}$). PET parameters were evaluated for correlations with outcome. **Results:** ^{18}F-FLT uptake decreased significantly between consecutive scans. An $SUV_{max(9)}$ decline $\geq$ 45% and a GTV_{VIS} decrease $\geq$ median during the first 2 treatment weeks were associated with better 3-y disease-free survival (88% vs. 63%, $P = 0.035$, and 91% vs. 65%, $P = 0.037$, respectively). A GTV_{VIS} decrease $\geq$ median in the fourth treatment week was also associated with better 3-y locoregional control (100% vs. 68%, $P = 0.021$). These correlations were most prominent in the subset of patients treated with chemoradiotherapy. Because of low ^{18}F-FLT uptake levels during treatment, GTV_{SBR} and $GTV_{50\%}$ were unsuccessful in segmenting primary tumor volume. **Conclusion:** In head and neck cancer, a change in ^{18}F-FLT uptake early during radiotherapy or chemoradiotherapy is a strong indicator for long-term outcome. ^{18}F-FLT PET may thus aid in personalized patient management by steering treatment modifications during an early phase of therapy.

Key Words: ^{18}F-fluorothymidine PET; head and neck cancer; early response monitoring

J Nucl Med 2013; 54:532–540
DOI: 10.2967/jnumed.112.105999

Received Mar. 14, 2012; revision accepted Sep. 20, 2012.
For correspondence or reprints contact: Bianca A.W. Hoeben, Department of Radiation Oncology 874, Radboud University Nijmegen Medical Centre, P.O. Box 9101, 6500 HB Nijmegen, The Netherlands.
E-mail: b.hoeben@rther.umcn.nl
*Contributed equally to this work.
Published online Jan. 23, 2013.

PET with the glucose analog ^{18}F-FDG is accepted as a powerful molecular imaging method exploiting the increased metabolic activity of cancer cells. ^{18}F-FDG PET has found its way into clinical practice for diagnosis and staging of various cancer types (*1,2*). However, interpretation of ^{18}F-FDG PET findings requires caution because of uptake in nonmalignant tissues caused by peritumoral inflammation and physiologic changes, especially in the head and neck region (*3,4*).

Enhanced proliferative activity is an even more characteristic feature of malignant lesions (*5*). Furthermore, especially in squamous cell carcinomas of the head and neck, compensatory tumor cell proliferation during treatment is a known mechanism adversely affecting outcome (*6*). Various treatment regimens have been developed trying to counteract this effect, such as accelerated radiotherapy (*7,8*), chemoradiotherapy (*9*), or radiotherapy combined with cetuximab (*10*), but they also induce increased side effects (*11*). Assays to monitor the proliferative activity of tumors before and during treatment may assist in better selection of patients and possibly also in modification of treatment strategy based on early assessment of response (*12*).

Thus, an imaging biomarker for PET selectively reflecting cellular proliferation could be of great clinical value (*13*). Shields et al. introduced the thymidine analog 3′-deoxy-3′-^{18}F-fluorothymidine (^{18}F-FLT) as a PET tracer exploiting the activity of the enzyme thymidine kinase 1 as a measure of proliferative activity (*14*). ^{18}F-FLT is phosphorylated by thymidine kinase 1 and trapped intracellularly (*14*). During DNA synthesis, thymidine kinase 1 activity increases almost 10-fold. ^{18}F-FLT trapping is related to thymidine kinase 1 activity and is a measure of proliferative activity (*15*). ^{18}F-FLT accumulation has been reported in various tumor types (*16*).

In a preclinical study, single-dose radiation significantly reduced ^{18}F-FLT uptake in murine SCCVII tumors, whereas no visible change in tumor size or morphology was noted (*17*). Also, in imaging studies of patients with head and neck cancer, the ^{18}F-FLT signal declined within

1–2 wk after the start of radiotherapy without apparent changes in tumor volume (*18,19*).

In this study, 48 patients with squamous cell carcinomas of the head and neck underwent consecutive ^{18}F-FLT PET/CT scanning before and during the course of radiotherapy or chemoradiotherapy to assess whether early changes in tumor uptake volume and signal seen on ^{18}F-FLT PET can predict long-term clinical outcome.

MATERIALS AND METHODS

Patients

Eligibility criteria included newly diagnosed squamous cell carcinoma of the head and neck, International Union Against Cancer stage II–IV (*20*), radiotherapy with or without concomitant chemotherapy with curative intent, an age of 18 y or older, and written informed consent. Exclusion criteria were surgery as primary tumor therapy, palliative treatment, and pregnancy. Inclusion lasted from July 2006 until August 2008. Follow-up was every 2 mo in the first year, every 3 mo in the second year, every 4 mo in the third year, and every 6 mo in the fourth and fifth years. At these visits, relevant medical history was taken and the head and neck region was fully examined (flexible endoscopy, palpation, and inspection). When residual or recurrent disease was suspected, further clinical and imaging diagnostics were performed. If a patient had been released from standard follow-up, information was sought by contacting the general practitioner or other medical specialists. Follow-up was censored on December 31, 2010. The Institutional Review Board of Radboud University Medical Centre Nijmegen approved the study.

Treatment

For 18 patients, 3-dimensional conformal radiotherapy was used, delivering a dose of 68 Gy in 2-Gy fractions to the primary tumor and metastatic cervical lymph nodes and 44 Gy to electively treated nodes. All other patients were treated with intensity-modulated radiation therapy with a simultaneous integrated boost technique, delivering a dose of 68 Gy in 2-Gy fractions to the primary tumor and metastatic cervical lymph nodes and 50.3 Gy in 1.48-Gy fractions to electively treated nodes. For all patients, an accelerated fractionation schedule was used with an overall treatment time of 5.5 wk, delivering 2 fractions daily during the last 1.5 wk of treatment. In accordance with institutional guidelines, 15 patients with advanced T3 and T4 tumors, less than 70 y old and without contraindications for cisplatinum administration, were concomitantly treated with intravenous cisplatinum, 40 mg/m^2, once weekly (Supplemental Fig. 1, available online at http://jnm.snmjournals.org).

^{18}F-FLT Synthesis

^{18}F-FLT was obtained from the Department of Nuclear Medicine and PET Research, Free University Medical Center, Amsterdam, The Netherlands. The synthesis method was described by Troost et al. (*18*).

^{18}F-FLT PET/CT Acquisition

Before the start of treatment, in the second week of treatment, and in the fourth week of treatment, integrated ^{18}F-FLT PET and CT images were acquired on a hybrid PET/CT scanner (Biograph Duo; Siemens/CTI). The PET acquisition method was described previously (*18*). All scans were obtained with the patient supine. An individual head support and a rigid customized mask covering the head and neck area were used to increase positioning accuracy and to reduce movement artifacts during image acquisition. Sixty minutes after intravenous injection of 250 MBq of ^{18}F-FLT, emission images of 2 bed positions over the head and neck area were recorded, with 7 min per bed position in 3-dimensional mode. The PET images were reconstructed using iterative ordered-subsets expectation maximization with the parameters optimized for the head and neck area (i.e., 4 iterations, 16 subsets, and a 5-mm 3-dimensional gaussian filter (*21*)) and with correction for photon attenuation (voxel size, 5.31 × 5.31 × 3.38 mm). Additionally, CT images were acquired for anatomic correlation and attenuation correction using 80 mAs and 130 kV (voxel size, 0.98 × 0.98 × 3.00 mm). For contrast enhancement, a 70-mL bolus of nonionic iodinated contrast agent (300 mg/mL) (ioversol, Optiray 300; Tyco Healthcare/Mallinckrodt Inc.) was given intravenously and the CT was performed with a 40-s delay in the venous phase.

^{18}F-FLT PET/CT Analysis

After reconstruction, standardized uptake value (SUV) PET images were created with in-house–developed software correcting for injected dose, tracer decay, and patient body weight. Subsequently, the images were resliced using the CT format as a reference. The SUV PET and CT images were then imported into the department's radiotherapy planning system, Pinnacle^3 (version 8.0 d; Philips Radiation Oncology Systems). With this software, consecutive CT and PET scans were registered to the first CT scan using rigid cross-correlation. Two investigators delineated the gross tumor volume of the primary tumor on the first CT scans in consensus using all available diagnostic clinical and imaging information. Tumor $SUV_{max(9)}$ was defined as mean uptake in the hottest voxel of the tumor and its 8 surrounding voxels in 1 transversal slice. Standard regions of interest in normal tissues (brain, parotid gland, tongue, neck musculature, and bone marrow of the third cervical vertebra) were delineated in each scan, at the same anatomic locations for every patient. From these regions of interest, mean SUV (SUV_{mean}) was calculated for interscan comparison.

PET Tumor Segmentation

Several segmentation methods were applied to the primary tumor volume on the ^{18}F-FLT PET images. Visual gross tumor volume (GTV_{VIS}) contouring of the ^{18}F-FLT PET images was performed by an experienced radiation oncologist who did not know the treatment outcome.

In addition, an adaptive threshold delineation based on the signal-to-background ratio was performed (GTV_{SBR}) using $SUV_{max(9)}$ (*22*). Mean background uptake was calculated from a manually defined region of interest in the neck musculature (~10 cm^3) at a sufficient distance from the vertebrae, the primary tumor, and lymph node metastases. A third method delineated the 50% isocontour of the maximum signal intensity in the tumor ($GTV_{50\%}$).

PET parameter differences between scans were calculated as absolute difference (scan 1 – scan 2) and relative difference [(scan 1 – scan 2)/scan 1]. The difference per radiotherapy fraction between scans was calculated [(scan 1 – scan 2)/number of fractions between scans] to investigate whether the number of fractions between scans confounded the analyses.

Statistical Analysis

The aim of this prospective study was to investigate whether changes in ^{18}F-FLT uptake during treatment can predict clinical outcome. When the study was designed in 2005, no formal power

analysis could be performed, since clinical data regarding the uptake of ^{18}F-FLT in advanced-stage head and neck cancer and regarding the degree of possible uptake changes during radiotherapy or chemoradiotherapy were lacking. It was anticipated that a cohort of 40 evaluable patients would suffice to indicate the value of ^{18}F-FLT PET for early response assessment. If this could not be demonstrated with 40 patients, the effect would probably not be of clinical relevance. To compensate for an estimated 25% of patients who would not be evaluable, the inclusion target was approximately 50 patients. Statistical analyses were performed using SPSS, version 16.0 (SPSS), and Prism, version 4.0c (GraphPad Software, Inc.). The Kolmogorov–Smirnov test was used to evaluate gaussian distribution. Correlation was determined by the Spearman test. Differences between paired parameters were tested by Wilcoxon signed-rank or *t* testing (2 groups) and the Friedman test (3 groups). Survival was calculated from the date of the first PET examination until the date of death or until censoring on the date of last follow-up. Three-year disease-free survival (DFS), locoregional control (LRC), and overall survival (OS) were analyzed using Kaplan–Meier estimates with the log-rank test for univariate comparison. Continuous variables were dichotomized at the median. When a cutoff at the median was not discriminative (in 2 instances), the most distinguishing cutoff was sought using receiver-operating-characteristic methodology optimizing specificity and sensitivity to obtain the highest accuracy.

A 2-sided *P* value of less than 0.05 was considered significant.

RESULTS

Patient Characteristics

Fifty-two patients with 54 tumors were accrued in the study. Four patients were excluded from evaluation because they were not treated according to the standard guideline but received experimental therapy. Forty-eight patients with 50 head and neck tumors were thus evaluable (Table 1). All patients underwent ^{18}F-FLT PET/CT before therapy (median, 4 d before first radiotherapy fraction; range, 0–14 d), and all but 2 patients underwent ^{18}F-FLT PET/CT in the second week (after a median of 7 fractions; range, 5–12 fractions). After an approved amendment of the study protocol, the subsequent 29 patients also underwent a third scan in the fourth week of treatment (after a median of 18 fractions; range, 15–19 fractions). The reason for this third scan was to investigate whether the substantial decrease in ^{18}F-FLT uptake after 1 wk continued or whether tumor cell repopulation occurring later during the course of treatment might increase ^{18}F-FLT uptake again. After completion of therapy, all patients showed a complete local response. All patients but one showed a clinical complete regional response. The patient with a residual cervical lymph node after radiotherapy underwent cervical lymph node dissection. Histology confirmed complete regional response, as only a 2.9-cm completely necrotic node was found. The patients were followed until death or for at least 2 y (median, 36 mo). The median follow-up time for all patients was 32 mo (range, 8–52 mo).

Clinical Characteristics and Outcome

The estimated 3-y OS rate was 78% (95% confidence interval [CI], 66%–90%), LRC was 84% (95% CI, 74%–95%), and DFS was 79% (95% CI, 67%–91%).

TABLE 1
Patient Characteristics and Events

Characteristic	Data
Age at baseline PET (y)	
Mean	60
Range	39–75
Sex (n = 48)	
Female	10 (21)
Male	38 (79)
Smoking (n = 48)	
Active	33 (69)
Former	12 (25)
Unknown	3 (6)
Alcohol use (n = 48)	
Active	35 (73)
Former	4 (8)
Never	4 (8)
Unknown	5 (10)
T stage (n = 50)	
1	1 (2)
2	25 (50)
3	17 (34)
4	7 (14)
N stage (n = 50)	
0	22 (44)
1	6 (12)
2a	—
2b	11(22)
2c	11 (22)
International Union Against Cancer stage (n = 50)	
II	12 (24)
III	13 (26)
IVA	25 (50)
Histologic grade (n = 50)	
1	4 (8)
2	26 (52)
3	11 (22)
Unknown	9 (18)
Primary tumor site (n = 50)	
Oral cavity	1 (2)
Oropharynx	27 (54)
Larynx	14 (28)
Hypopharynx	8 (16)
Treatment (n = 48)	
Radiotherapy	33 (69)
Chemoradiotherapy	15 (31)
No. of events tumor-related (n = 48)	
Locoregional recurrence	7 (15)
Distant metastases*	4 (8)
Tumor-related death	7 (15)
No. of events not tumor-related (n = 48)	
Death due to another cause	6 (13)
Second primary tumor after start of study†	8 (17)

*Distant metastases (pulmonal, skeletal, cerebral, and cutaneous) were detected after 7, 9, and 11 mo.

†Second primary tumors were located in head and neck area, lungs, esophagus, rectum, bladder, and skin.

Data are numbers of patients, with percentages in parentheses, except for age, which is years.

As expected, patients with a more advanced T- or N-stage had worse LRC (3-y LRC for T3 vs. T4, 100% [95% CI, 80–100] vs. 57% [95% CI, 20–94], $P = 0.004$; 3-y LRC for N0–N1 vs. N2c, 91% [95% CI, 80–100] vs. 64% [95% CI, 35–92], $P = 0.028$). Also, younger people (<60 y) had significantly worse LRC (3-y LRC, 73% [95% CI, 55–92] vs. 96% [95% CI, 88–100], $P = 0.041$). Histologic tumor grade and therapy regimen were not significantly predictive for outcome.

In the correlation of clinical characteristics with baseline PET/CT parameters, T-stage was only moderately correlated with segmented GTVs on CT and PET (Spearman $r = 0.34–0.42$; $P = 0.003–0.007$). No correlation was found between PET or CT parameters and nodal stage, tumor differentiation, or primary tumor location.

Baseline PET Parameters and Outcome

CT and PET tumor volumes did not correlate with $SUV_{max(9)}$.

Smaller tumors on CT (<6.5 cm^3) showed significantly better LRC in the whole group and in the subgroup of radiotherapy patients (Table 2). In line with CT volume, patients displaying a GTV_{VIS} of less than 6.5 cm^3 showed better LRC, although this difference was not statistically significant.

Initially, all tumors displayed ^{18}F-FLT uptake. In patients treated with only radiotherapy, a baseline-scan $SUV_{max(9)}$ below 6.6 predicted better LRC and significantly better DFS than did a baseline $SUV_{max(9)}$ above 6.6. In contrast, in patients receiving chemoradiotherapy, an initial $SUV_{max(9)}$

TABLE 2
Outcome as Function of (Changes in) PET/CT Parameters

Parameter	Best group by cutoff level	*P*		
		3-y LRC	3-y DFS	3-y OS
All patients				
$SUV_{max(9)}$ 1	$SUV_{max(9)} \geq 6.1$*	0.17	0.12	0.52
GTV_{CT} 1	$GTV_{CT} < 6.5$ cm^3	100 (80–100) vs. 76 (60–92): 0.044†	0.27	0.13
GTV_{VIS} 1	$GTV_{VIS} < 6.5$ cm^3	100 (75–100) vs. 79 (65–93): 0.092	0.20	0.26
Δ $SUV_{max(9)}$ 1–2	Decrease ≥ 45%‡	92 (80–100) vs. 72 (51–93): 0.066	88 (75–100) vs. 63 (41–85): 0.035†	0.23
Δ GTV_{VIS} 1–2	Decrease ≥ 41%*	0.21	91 (80–100) vs. 65 (46–84): 0.037†	0.86
Δ GTV_{VIS} 1–3	Decrease ≥ 78%*	100 (78–100) vs. 68 (41–94): 0.021†	100 (78–100) vs. 56 (30–83): 0.005†	80 (54–100) vs. 48 (6–89): 0.084
Radiotherapy				
$SUV_{max(9)}$ 1	$SUV_{max(9)} < 6.6$‡	95 (85–100) vs. 70 (41–99): 0.075	90 (77–100) vs. 59 (31–87): 0.044†	0.59
GTV_{CT} 1	$GTV_{CT} < 6.5$ cm^3	100 (79–100) vs. 73 (50–96): 0.048†	0.26	0.25
GTV_{VIS} 1	$GTV_{VIS} < 6.5$ cm^3	0.11	0.20	0.44
Δ $SUV_{max(9)}$ 1–2	Decrease ≥ 45%	0.48	0.20	0.65
Δ GTV_{VIS} 1–2	Decrease ≥ 47%*	0.95	0.20	0.27
Δ GTV_{VIS} 1–3	Decrease > 77%*	100 (72–100) vs. 66 (34–98): 0.05	100 (72–100) vs. 53 (23–83): 0.013†	0.12
Chemoradiotherapy				
$SUV_{max(9)}$ 1	$SUV_{max(9)} \geq 6.6$*	100 (63–100) vs. 57 (20–94): 0.044†	100 (63–100) vs. 57 (20–94): 0.044†	100 (63–100) vs. 57 (8–100): 0.080
GTV_{CT} 1	$GTV_{CT} < 6.5$ cm^3	0.63	0.63	0.66
GTV_{VIS} 1	$GTV_{VIS} < 6.5$ cm^3	0.63	0.63	0.66
Δ $SUV_{max(9)}$ 1–2	Decrease ≥ 45%	100 (54–100) vs. 57 (20–94): 0.081	100 (54–100) vs. 57 (20–94): 0.081	100 (54–100) vs. 57 (8–100): 0.10
Δ GTV_{VIS} 1–2	Decrease ≥ 31%*	100 (59–100) vs. 50 (10–90): 0.039†	100 (59–100) vs. 50 (10–90): 0.039†	100 (59–100) vs. 56 (7–100): 0.079
Δ GTV_{VIS} 1–3	Not tested§	Not tested§	Not tested§	Not tested§

*Dichotomization by median value.
†$P < 0.05$.
‡Dichotomization value found through receiver-operating-characteristic analysis.
§Too few subjects for testing ($n = 7$).
GTV_{CT} = visually delineated gross tumor volume on CT; Δ = difference between baseline scans (1) and subsequent scans (2 or 3).
Numbers after PET/CT parameters refer to first, second, or third scan. For survival data with $P \leq 0.1$, 3-y survival data per group are given (%), with 95% CI in parentheses; for survival differences with $P > 0.1$, only *P* value is given.

below 6.6 predicted worse LRC, DFS, and OS than did an $SUV_{max(9)}$ above 6.6, though the difference in OS did not reach statistical significance. For the entire group, $SUV_{max(9)}$ dichotomized at the median was not significantly predictive for outcome (Table 2).

Changes in $SUV_{max(9)}$ and GTV During Therapy and Relation with Outcome

Relative to the baseline scan, there was a significant decrease in mean (±SD) $SUV_{max(9)}$ (46.0% ± 26.9 vs. 69.8% ± 13.5, Friedman $P < 0.0001$) and GTV_{VIS} (33.2% ± 46.9 vs. 67.8% ± 29.8, Friedman $P < 0.0001$) on the scans obtained in the second and fourth weeks of therapy (Figs. 1 and 2). These decreases remained statistically significant when the groups of patients treated with radiotherapy or chemoradiotherapy were analyzed separately. In contrast, no overall significant change in GTV_{SBR} was observed, and $GTV_{50\%}$ even demonstrated an increase in the fourth week. The reason for these latter findings was the large decrease in $SUV_{max(9)}$ that had already occurred in the second week of treatment, with the 50% isocontour approaching the level of the background signal. Consequently, the GTV_{SBR} and $GTV_{50\%}$ methods became less sensitive for discriminating tumor signal from background. For this reason, GTV_{SBR} and $GTV_{50\%}$ were not used for further analysis.

For associations with outcome, both absolute and relative changes in PET parameters were analyzed, with nearly identical results. Therefore, only the results from the relative change analysis will be presented. The number of radiotherapy fractions that patients received between scans did not confound the outcome of the scan parameter analysis.

An $SUV_{max(9)}$ decrease ≥ 45% during the first 2 wk of treatment was associated with a significantly better DFS (88% [95% CI, 75–100] vs. 63% [95% CI, 41–85], $P = 0.035$; Fig. 3). In the fourth week of treatment, $SUV_{max(9)}$ in all patients had decreased to such an extent that it was no longer discriminative for outcome (Table 2).

A GTV_{VIS} decrease above median between the baseline scan and the 2 subsequent scans was associated with significantly better LRC and DFS (Table 2 and Fig. 4). The association was most pronounced in the group of chemoradiotherapy patients, with a DFS of 100% (95% CI, 59–100) for those with a ≥31% (median) decrease after 2 wk of treatment versus 50% (95% CI, 10–90) for those with a <31% decrease ($P = 0.039$, Fig. 4C). For the radiotherapy-only group, a statistically significant effect was not reached until the fourth week of treatment.

Normal Tissues

^{18}F-FLT uptake in normal tissues did not significantly differ from baseline in subsequent scans, underlining the reproducibility of the imaging method over time. The mean parotid gland SUV_{mean} was 0.8 ± 0.2 in the baseline scan, 0.8 ± 0.2 in scan 2, and 0.7 ± 0.2 in scan 3. For muscle uptake, these values were 0.6 ± 0.1, 0.6 ± 0.1, and 0.5 ± 0.1, respectively. For brain tissue, mean SUV_{mean} was 0.3 ± 0.1, 0.2 ± 0.1, and 0.2 ± 0.0, respectively. Tongue tissue values were 0.7 ± 0.2, 0.7 ± 0.2, and 0.6 ± 0.1, respectively. As expected, only the bone marrow in the cervical vertebra (being a highly proliferative tissue affected by radiotherapy) showed a significant decrease in ^{18}F-FLT uptake (Fig. 2). Mean SUV_{mean} of the third cervical vertebra changed from 2.8 ± 0.8 to 0.5 ± 0.1 to 0.4 ± 0.1, respectively ($P < 0.01$ for difference between scans after paired-samples t testing and Bonferroni adjustments).

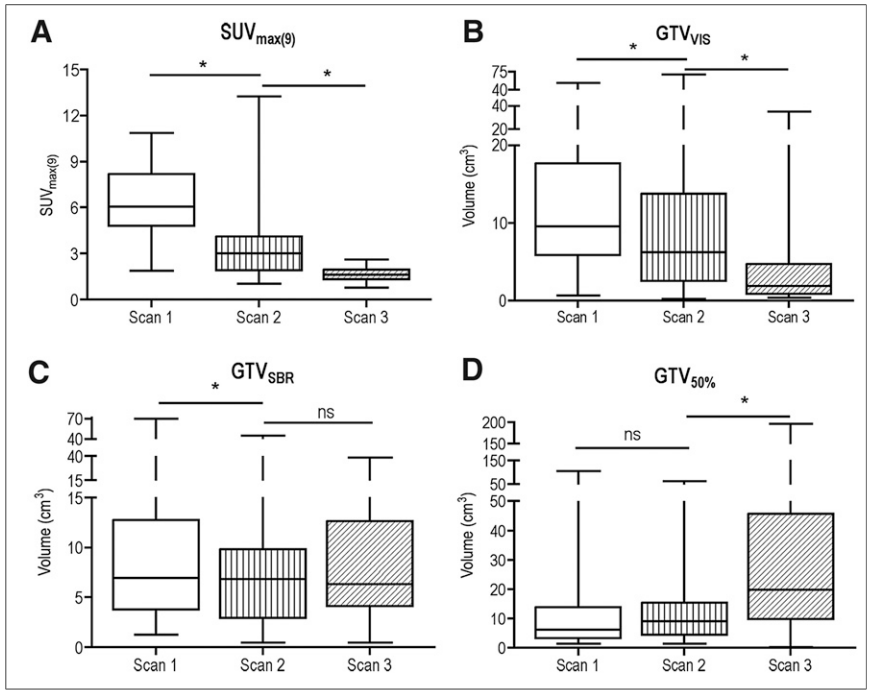

FIGURE 1. Box plots of $SUV_{max(9)}$ (A), GTV_{VIS} (B), GTV_{SBR} (C), and $GTV_{50\%}$ (D) on consecutive ^{18}F-FLT PET/CT scans. Bottom and top of each box are lower and upper quartiles. Black band near middle of box is median. Extremes of lower and higher whiskers represent range of minimum and maximum values. *$P \leq 0.001$, Wilcoxon signed-rank test.

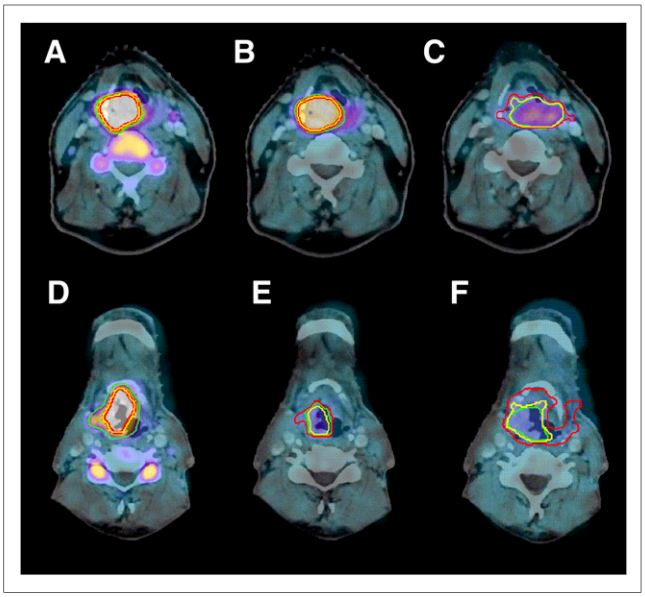

FIGURE 2. ^{18}F-FLT PET/CT before therapy (A and D), in second week of therapy (B and E), and in fourth week of therapy (C and F). First example (A–C) shows slow decrease in ^{18}F-FLT uptake (cT4N2bM0 supraglottic laryngeal carcinoma treated with chemoradiotherapy; local recurrence after 7 mo; later distant metastases) and second one (D–F) fast decrease (cT3N1M0 supraglottic laryngeal carcinoma treated with radiotherapy only; no tumor-related event after 32 mo of follow-up). For GTV_{VIS} (green), 3-dimensional volume change was +8% between A and B, −35% between A and C, −60% between D and E, and −66% between D and F. For GTV_{SBR} (yellow), 3-dimensional volume change was +7% between A and B, +4% between A and C, −44% between D and E, and +22% between D and F. For $GTV_{50\%}$ (red), 3-dimensional volume change was +11% between A and B, +102% between A and C; +30% between D and E, and +247% between D and F. $SUV_{max(9)}$ changed by −35% between A and B, −70% between A and C, −58% between D and E, and −69% between D and F.

DISCUSSION

Accelerated tumor cell repopulation is an important cause of treatment failure in head and neck cancer (*6*). Visualization of the proliferative tumor cell compartment and early modification of treatment to counteract this resistance mechanism can help improve outcome. Decisions for more aggressive therapy, such as chemoradiotherapy, accelerated radiotherapy, or a combination of radiotherapy with cetuximab to counteract proliferation, are currently driven by clinical and radiologic tumor characteristics and by patient factors. In individualized therapy strategies, additional information from ^{18}F-FLT PET could be of complementary value in intensifying treatment if needed and, possibly, in deescalating treatment when early evaluation indicates high responsiveness.

In this study, patients with head and neck tumors were prospectively evaluated with repetitive ^{18}F-FLT PET/CT before and early during therapy, to analyze associations between scan findings and clinical outcome after prolonged follow-up. In patients who are routinely treated with radiotherapy, a pretreatment ^{18}F-FLT PET scan with a high $SUV_{max(9)}$ (>6.6) predicts poor outcome and thus could sway the decision toward the addition of chemotherapy to reduce the observed high proliferation rate. This is strengthened by the observation that in the group of patients treated with concurrent chemoradiotherapy, a pretreatment $SUV_{max(9)}$ higher than 6.6 was associated with better outcome, suggesting that the addition of chemotherapy might be particularly relevant for highly proliferative tumors. Chemotherapy most likely enhances the antiproliferative effect of the accelerated irradiation schedule, ultimately resulting in improved treatment outcome.

Serial PET/CT of ^{18}F-FLT demonstrated a decrease in proliferative activity during therapy, as reported earlier in a radiotherapy dose–planning exercise that included 10 patients of the current study cohort (*18*). Greater decline in tumor uptake was predictive of better clinical outcome in DFS and LRC, with a particularly strong early association in the patients treated with chemoradiotherapy. A possible limitation to this study is that, even though ^{18}F-FLT PET/CT parameters displayed a clear prognostic potential on univariate analysis, a robust multivariate analysis correcting for various clinical and pathologic variables was precluded by the relatively small study population with too few outcome events.

As to the timing of ^{18}F-FLT PET scans during therapy, the results suggest that evaluation is best done in the second week of treatment. Later measurements did not add much information, and the ^{18}F-FLT PET signal became more difficult to quantify because of decreasing signal-to-noise ratios. In addition, if adjustments of the treatment strategy are anticipated, these should be decided as early as possible after the start of therapy.

Early evaluation of the response to therapy has been assessed using ^{18}F-FLT PET in several malignancies (*23–32*). In 30 patients with recurrent glioma treated with bevacizumab, changes in ^{18}F-FLT uptake after 6 wk of treatment were predictive for patient outcome, with a median OS 3.3 times longer in PET responders than in nonresponders. Assessment

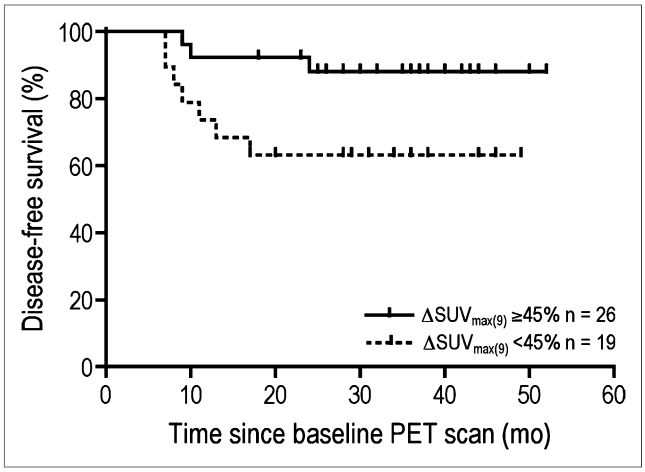

FIGURE 3. $SUV_{max(9)}$ above or below 45% decrease between scans 1 and 2 for entire group of patients. $P = 0.035$.

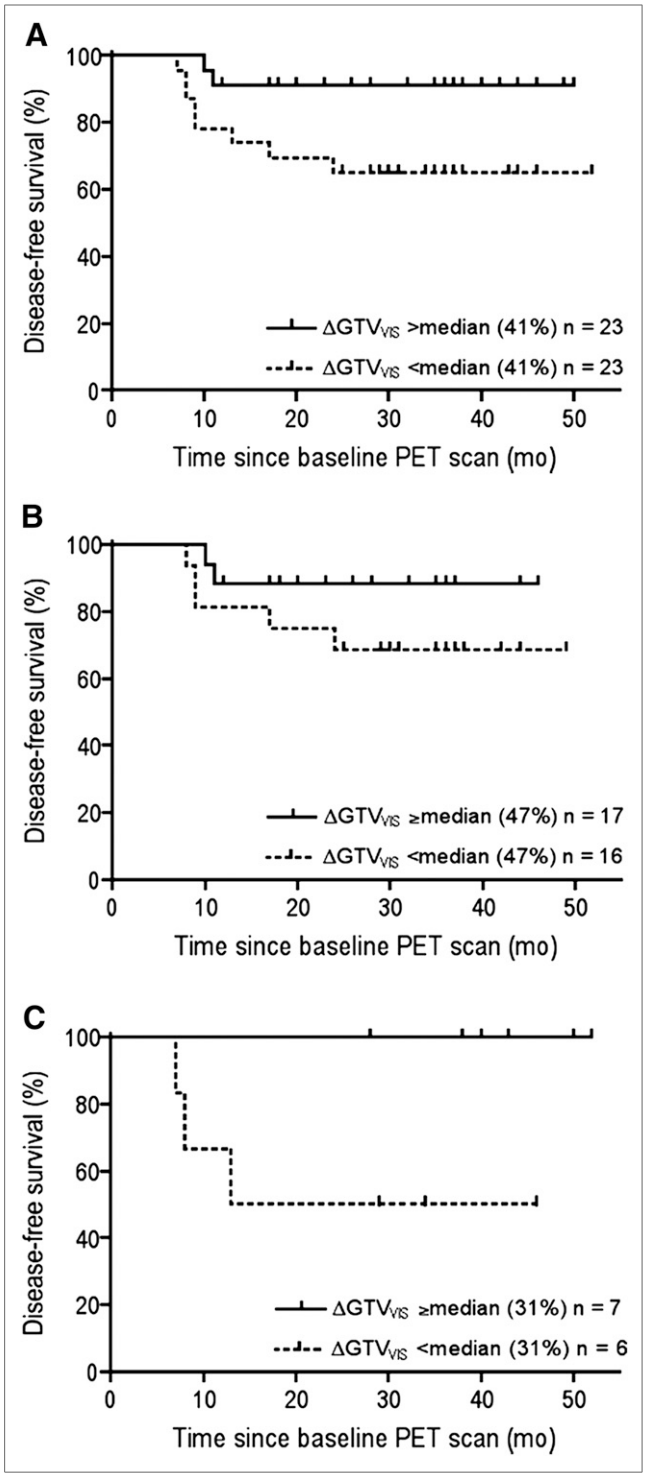

FIGURE 4. GTV_{VIS} decrease above or below median between scans 1 and 2 for all patients (A), radiotherapy group (B), and chemoradiotherapy group (C). $P = 0.037$, 0.203, and 0.039, respectively.

of response using PET was superior to that using MR imaging (*28*). In a study of 34 patients with stage IV non–small cell lung carcinoma treated with erlotinib, Zander et al. demonstrated that ^{18}F-FLT PET can predict progression-free survival (*32*). In contrast, in a study of 10 patients with advanced rectal cancer, no direct relationship was found between a decrease in ^{18}F-FLT PET signal during neoadjuvant chemoradiotherapy and histopathologic tumor regression after resection (*29*).

Overall, the published data on ^{18}F-FLT PET for early response evaluation in most solid tumor types concur that a greater decrease in ^{18}F-FLT uptake is associated with a better treatment response. However, all previous studies have been performed either in palliative situations or with limited numbers of patients. Furthermore, most have had a relatively short follow-up and endpoints with less relevance for a curative situation (e.g., response according to the Response Evaluation Criteria in Solid Tumors). The current study had a larger cohort, with well-defined endpoints (LRC and DFS) and adequate follow-up (minimum of 2 y for surviving patients). In head and neck cancer, most recurrences are diagnosed within 2 y after treatment.

Previous studies on often nonuniformly treated cohorts of patients with head and neck cancer reported the prognostic potential for the more commonly used PET tracer ^{18}F-FDG (*33–35*). High pretreatment ^{18}F-FDG uptake was associated with poor outcome. There are several reports in the literature concerning the utility of ^{18}F-FDG PET/CT in providing prognostic information and as a tool for assessing treatment response 3 mo after completion of radiotherapy or chemoradiotherapy in patients with head and neck cancer (*36,37*). However, posttherapy assessment is useless when one is aiming for early treatment modification to improve outcome or reduce overtreatment. One recent study on 37 patients with head and neck cancer treated with chemoradiotherapy found associations between changes in ^{18}F-FDG uptake during therapy and tumor control (*38*). Another group did not observe this correlation after 2 wk of chemoradiotherapy in 26 patients with head and neck squamous cell carcinoma but found a prognostic value for ^{18}F-FDG PET/CT performed 8–12 wk after therapy with regard to disease-specific survival and relapse-free survival (*39*). Although a previous study showed that untreated laryngeal squamous cell tumors displayed a higher uptake of ^{18}F-FDG than of ^{18}F-FLT (*40*), all analyzed tumors in the current study, in different locations in the head and neck area, showed clearly discernable and quantifiable ^{18}F-FLT uptake on pretreatment PET scans. Moreover, ^{18}F-FLT uptake reduction could be followed during treatment, whereas (radiotherapy-induced) peritumoral mucosal inflammation may result in false-positive ^{18}F-FDG PET readings and can hamper accurate tumor volume measurements for this tracer.

In this study, 2 automatic or semiautomatic segmentation methods were applied for delineation of tumor volumes on the repetitive ^{18}F-FLT PET scans. GTVs defined using the signal-to-background ratio and the 50% isocontour of the maximum signal could not accurately define tumor areas during therapy because of the deteriorating signal-to-noise ratio and 50% isocontours approaching the background

level. During treatment, GTV_{VIS} reduction was prognostic for treatment outcome. However, since visual delineation is subject to applied window-level settings and the physician's expertise, operator-independent (automated) segmentation algorithms are required. This is a topic of current research.

CONCLUSION

This study demonstrated uptake of the proliferation PET tracer ^{18}F-FLT in all studied head and neck squamous cell cancers and a significant decrease in tracer uptake during the first 4 wk of radiotherapy or chemoradiotherapy. A greater decrease in ^{18}F-FLT uptake in the second week of treatment predicted a more favorable long-term outcome. Given the notion that tumor cell proliferation is a mechanism of therapy resistance, ^{18}F-FLT PET should provide an effective tool for decisions on early and personalized treatment adaptation in patients with head and neck cancer.

DISCLOSURE

The costs of publication of this article were defrayed in part by the payment of page charges. Therefore, and solely to indicate this fact, this article is hereby marked "advertisement" in accordance with 18 USC section 1734. This work was supported by EC FP6 funding (Biocare contract LSHC-CT-2004-505785) and by Junior Investigator Grant 2006-38 awarded by the Radboud University Nijmegen Medical Centre. No other potential conflict of interest relevant to this article was reported.

ACKNOWLEDGMENTS

We thank the technologists of the Departments of Radiation Oncology and Nuclear Medicine for their excellent assistance. Dr. John Lee from Université Catholique de Louvain, Belgium, is acknowledged for his kind permission to use the signal-to-background algorithm.

REFERENCES

1. Fletcher JW, Djulbegovic B, Soares HP, et al. Recommendations on the use of ^{18}F-FDG PET in oncology. *J Nucl Med.* 2008;49:480–508.
2. Bussink J, Kaanders JH, van der Graaf WT, Oyen WJ. PET-CT for radiotherapy treatment planning and response monitoring in solid tumors. *Nat Rev Clin Oncol.* 2011;8:233–242.
3. Strauss LG. Fluorine-18 deoxyglucose and false-positive results: a major problem in the diagnostics of oncological patients. *Eur J Nucl Med.* 1996;23:1409–1415.
4. Troost EG, Schinagl DA, Bussink J, et al. Innovations in radiotherapy planning of head and neck cancers: role of PET. *J Nucl Med.* 2010;51:66–76.
5. Buck AK, Schirrmeister H, Hetzel M, et al. 3-deoxy-3-[^{18}F]fluorothymidine-positron emission tomography for noninvasive assessment of proliferation in pulmonary nodules. *Cancer Res.* 2002;62:3331–3334.
6. Kim JJ, Tannock IF. Repopulation of cancer cells during therapy: an important cause of treatment failure. *Nat Rev Cancer.* 2005;5:516–525.
7. Fu KK, Pajak TF, Trotti A, et al. A Radiation Therapy Oncology Group (RTOG) phase III randomized study to compare hyperfractionation and two variants of accelerated fractionation to standard fractionation radiotherapy for head and neck squamous cell carcinomas: first report of RTOG 9003. *Int J Radiat Oncol Biol Phys.* 2000;48:7–16.
8. Overgaard J, Hansen HS, Specht L, et al. Five compared with six fractions per week of conventional radiotherapy of squamous-cell carcinoma of head and neck: DAHANCA 6 and 7 randomised controlled trial. *Lancet.* 2003;362:933–940.
9. Blanchard P, Baujat B, Holostenco V, et al. Meta-analysis of chemotherapy in head and neck cancer (MACH-NC): a comprehensive analysis by tumour site. *Radiother Oncol.* 2011;100:33–40.
10. Bonner JA, Harari PM, Giralt J, et al. Radiotherapy plus cetuximab for squamous-cell carcinoma of the head and neck. *N Engl J Med.* 2006;354:567–578.
11. Rütten H, Pop LA, Janssens GO, et al. Long-term outcome and morbidity after treatment with accelerated radiotherapy and weekly cisplatin for locally advanced head-and-neck cancer: results of a multidisciplinary late morbidity clinic. *Int J Radiat Oncol Biol Phys.* 2011;81:923–929.
12. Bussink J, van Herpen CM, Kaanders JH, Oyen WJ. PET-CT for response assessment and treatment adaptation in head and neck cancer. *Lancet Oncol.* 2010;11:661–669.
13. Shields AF, Grierson JR, Kozawa SM, Zheng M. Development of labeled thymidine analogs for imaging tumor proliferation. *Nucl Med Biol.* 1996;23:17–22.
14. Shields AF, Grierson JR, Dohmen BM, et al. Imaging proliferation in vivo with [F-18]FLT and positron emission tomography. *Nat Med.* 1998;4:1334–1336.
15. Rasey JS, Grierson JR, Wiens LW, Kolb PD, Schwartz JL. Validation of FLT uptake as a measure of thymidine kinase-1 activity in A549 carcinoma cells. *J Nucl Med.* 2002;43:1210–1217.
16. Bading JR, Shields AF. Imaging of cell proliferation: status and prospects. *J Nucl Med.* 2008;49(suppl 2):64S–80S.
17. Yang YJ, Ryu JS, Kim SY, et al. Use of 3′-deoxy-3′-[^{18}F]fluorothymidine PET to monitor early responses to radiation therapy in murine SCCVII tumors. *Eur J Nucl Med Mol Imaging.* 2006;33:412–419.
18. Troost EG, Bussink J, Hoffmann AL, Boerman OC, Oyen WJ, Kaanders JH. ^{18}F-FLT PET/CT for early response monitoring and dose escalation in oropharyngeal tumors. *J Nucl Med.* 2010;51:866–874.
19. Menda Y, Boles Ponto LL, Dornfeld KJ, et al. Kinetic analysis of 3′-deoxy-3′-^{18}F-fluorothymidine (^{18}F-FLT) in head and neck cancer patients before and early after initiation of chemoradiation therapy. *J Nucl Med.* 2009;50:1028–1035.
20. Sobin L, Wittekind C. *2002 UICC: TNM Classification of Malignant Tumours.* 6th ed. New York, NY: Wiley-Liss; 2002:19–42.
21. Vogel WV, Wensing BM, van Dalen JA, Krabbe PF, van den Hoogen FJ, Oyen WJ. Optimised PET reconstruction of the head and neck area: improved diagnostic accuracy. *Eur J Nucl Med Mol Imaging.* 2005;32:1276–1282.
22. Daisne JF, Sibomana M, Bol A, Doumont T, Lonneux M, Gregoire V. Tri-dimensional automatic segmentation of PET volumes based on measured source-to-background ratios: influence of reconstruction algorithms. *Radiother Oncol.* 2003;69:247–250.
23. Everitt S, Hicks RJ, Ball D, et al. Imaging cellular proliferation during chemoradiotherapy: a pilot study of serial ^{18}F-FLT positron emission tomography/computed tomography imaging for non-small-cell lung cancer. *Int J Radiat Oncol Biol Phys.* 2009;75:1098–1104.
24. Kenny L, Coombes RC, Vigushin DM, Al-Nahhas A, Shousha S, Aboagye EO. Imaging early changes in proliferation at 1 week post chemotherapy: a pilot study in breast cancer patients with 3′-deoxy-3′-[^{18}F]fluorothymidine positron emission tomography. *Eur J Nucl Med Mol Imaging.* 2007;34:1339–1347.
25. Soloviev D, Lewis D, Honess D, Aboagye E. [^{18}F]FLT: an imaging biomarker of tumour proliferation for assessment of tumour response to treatment. *Eur J Cancer.* 2012;48:416–424.
26. Mileshkin L, Hicks RJ, Hughes BG, et al. Changes in ^{18}F-fluorodeoxyglucose and ^{18}F-fluorodeoxythymidine positron emission tomography imaging in patients with non-small cell lung cancer treated with erlotinib. *Clin Cancer Res.* 2011;17:3304–3315.
27. Pio BS, Park CK, Pietras R, et al. Usefulness of 3′-[F-18]fluoro-3′-deoxythymidine with positron emission tomography in predicting breast cancer response to therapy. *Mol Imaging Biol.* 2006;8:36–42.
28. Schwarzenberg J, Czernin J, Cloughesy TF, et al. 3′-deoxy-3′-^{18}F-fluorothymidine PET and MRI for early survival predictions in patients with recurrent malignant glioma treated with bevacizumab. *J Nucl Med.* 2012;53:29–36.
29. Wieder HA, Geinitz H, Rosenberg R, et al. PET imaging with [^{18}F]3′-deoxy-3′-fluorothymidine for prediction of response to neoadjuvant treatment in

patients with rectal cancer. *Eur J Nucl Med Mol Imaging.* 2007;34:878–883.
30. Yue J, Chen L, Cabrera AR, et al. Measuring tumor cell proliferation with ^{18}F-FLT PET during radiotherapy of esophageal squamous cell carcinoma: a pilot clinical study. *J Nucl Med.* 2010;51:528–534.
31. Sohn HJ, Yang YJ, Ryu JS, et al. [^{18}F]fluorothymidine positron emission tomography before and 7 days after gefitinib treatment predicts response in patients with advanced adenocarcinoma of the lung. *Clin Cancer Res.* 2008;14:7423–7429.
32. Zander T, Scheffler M, Nogova L, et al. Early prediction of nonprogression in advanced non-small-cell lung cancer treated with erlotinib by using [^{18}F]fluorodeoxyglucose and [^{18}F]fluorothymidine positron emission tomography. *J Clin Oncol.* 2011;29:1701–1708.
33. Allal AS, Slosman DO, Kebdani T, Allaoua M, Lehmann W, Dulguerov P. Prediction of outcome in head-and-neck cancer patients using the standardized uptake value of 2-[^{18}F]fluoro-2-deoxy-D-glucose. *Int J Radiat Oncol Biol Phys.* 2004;59:1295–1300.
34. Kim SY, Roh J-L, Kim MR, et al. Use of ^{18}F-FDG PET for primary treatment strategy in patients with squamous cell carcinoma of the oropharynx. *J Nucl Med.* 2007;48:752–757.
35. Schwartz DL, Rajendran J, Yueh B, et al. FDG-PET prediction of head and neck squamous cell cancer outcomes. *Arch Otolaryngol Head Neck Surg.* 2004;130:1361–1367.
36. Murphy JD, La TH, Chu K, et al. Postradiation metabolic tumor volume predicts outcome in head-and-neck cancer. *Int J Radiat Oncol Biol Phys.* 2011;80:514–521.
37. Isles MG, McConkey C, Mehanna HM. A systematic review and meta-analysis of the role of positron emission tomography in the follow up of head and neck squamous cell carcinoma following radiotherapy or chemoradiotherapy. *Clin Otolaryngol.* 2008;33:210–222.
38. Hentschel M, Appold S, Schreiber A, et al. Early FDG PET at 10 or 20 Gy under chemoradiotherapy is prognostic for locoregional control and overall survival in patients with head and neck cancer. *Eur J Nucl Med Mol Imaging.* 2011;38:1203–1211.
39. Castaldi P, Rufini V, Bussu F, et al. Can "early" and "late" ^{18}F-FDG PET-CT be used as prognostic factors for the clinical outcome of patients with locally advanced head and neck cancer treated with radio-chemotherapy? *Radiother Oncol.* 2012;103:63–68.
40. Cobben DC, van der Laan BF, Maas B, et al. ^{18}F-FLT PET for visualization of laryngeal cancer: comparison with ^{18}F-FDG PET. *J Nucl Med.* 2004;45:226–231.